

Physics 405 - Experiment 5: Hyperfine Structure of Rubidium

Dillon Walton

March 2023

Introduction

In this experiment, atomic spectroscopy is performed using a DBR diode laser to investigate the hyperfine structure splitting of rubidium at room temperature. The diode laser is calibrated to 780 nm wavelength in order to probe the $5S_{1/2}$ to $5P_{3/2}$ transition. By oscillating the laser frequency around the resonance transition frequencies of the atom and measuring the laser intensity, a measurement for the mean temperature of the atoms is obtained. A final temperature reading of $439K$ was obtained, which is significantly higher than expected. These results suggest an error in the analysis or a source of systematic error which was unaccounted for. An explanation of theory, experimental setup, results and conclusions follow in the sections below. Additionally, suggestions for further improvements to the experiment are made.

1 Theory

Bohr's quantum theory was originated by considering the hydrogen atom and postulating the quantization of energy levels. This model, as described in equation (1), describes the energy levels, or states, at which an electron can exist in the hydrogen atom.

$$E_n = \frac{-2\pi^2 me^4}{n^2 h^2} \quad (1)$$

They are discrete and therefore electrons cannot exist in between two states, which is where quantum mechanics breaks from the continuous nature of classical mechanics.

Fine structure splitting and hyperfine structure splitting arise from the quantization of angular momentum. The fine structure splitting comes from the interaction of the spin, \mathbf{S} , of an electron and the magnetic field, \vec{B} , of the nucleus. In the rest frame of an electron, the nucleus is orbiting around it, carrying charge and therefore creating a magnetic field proportional to the orbital angular momentum, \mathbf{L} , of the nucleus. The total angular momentum, $\mathbf{J} = \mathbf{S} + \mathbf{L}$, can thus take on several discrete values based on \mathbf{S} and \mathbf{L} of the atom. Each possible value splits the energy of a given quantum state, n , into further discrete values which we describe as fine structure splitting of energy levels.

The hyperfine structure splitting arises from considering the rest frame of the nucleus. In this frame, an electron is orbiting the nucleus with a given orbital angular momentum, proportional to \mathbf{J} , and creating a magnetic field, \vec{B} . The nucleus also has a spin, \mathbf{I} , which couples to the magnetic field of the electron. Again, the total angular momentum, $\mathbf{F} = \mathbf{I} + \mathbf{J}$, is quantized and will split the energy of the quantum state into further discrete energy levels. The hyperfine structure splitting is much smaller than the fine structure splitting as a result of the mass of the nucleus being much greater than the electron, therefore its magnetic moment is much smaller.

In this experiment, we focus on the hyperfine structure splitting of rubidium (Rb). Natural rubidium is composed of two isotopes, ^{87}Rb and ^{85}Rb with a distribution of approximately 28% and 72%, respectively [2]. The atomic structure of these two isotopes is largely the same with $Z = 37$, however ^{87}Rb contains two more neutrons than ^{85}Rb and therefore has a higher mass [7, 8]. The different structure of the nucleus additionally gives rise to a difference in the nuclear spin of the isotopes, \mathbf{I} , and therefore affects the hyperfine structure we observe. Rubidium is a convenient to study due to its single valence electron in the $n = 5$ state, which allows us to use the Bohr model to describe its energies [6]. To find the shift in energy which arises from the hyperfine splitting, and therefore the frequencies of light which the atom will absorb, we consider the different values \mathbf{F} can have.

To calculate \mathbf{F} , we consider \mathbf{J} and \mathbf{I} . For the $5^2S_{1/2}$, $\mathbf{J} = 1/2$ and $\mathbf{I} = 3/2$ for ^{85}Rb , and $\mathbf{J} = 1/2$ and $\mathbf{I} = 5/2$ for ^{87}Rb [6]. The hyperfine energy shift of this state for both isotopes is given in equation (2).

$$\Delta E_{hf} = \frac{1}{2} h A [\mathbf{F}(\mathbf{F} + 1) - \mathbf{J}(\mathbf{J} + 1) - \mathbf{I}(\mathbf{I} + 1)] \quad (2)$$

Where h is Planck's constant and A is a coupling coefficient. When a source of energy equal to the hyperfine energy shift of the isotope is applied, the energy will be absorbed and the valence electron will rise to an excited state. This energy difference is observed in this experiment.

2 Experimental Setup

The method used to investigate the hyperfine structure of atoms is atomic spectroscopy. By using a known energy source such as a laser, and focusing it to an atom, the frequencies of light which the atom absorbs energy can be observed and the structure of the atom can be determined. In this experiment, a diode laser is applied to a cell of rubidium vapor before reaching a photodiode, where the intensity of the laser is recorded. The use of the diode laser in this experiment provides a monochromatic and steady source of energy with which to probe the atom. The technology of the laser is based on stimulated emission, which allows us to adjust the wavelength of the laser by changing the temperature and current supplied to the diode [6].

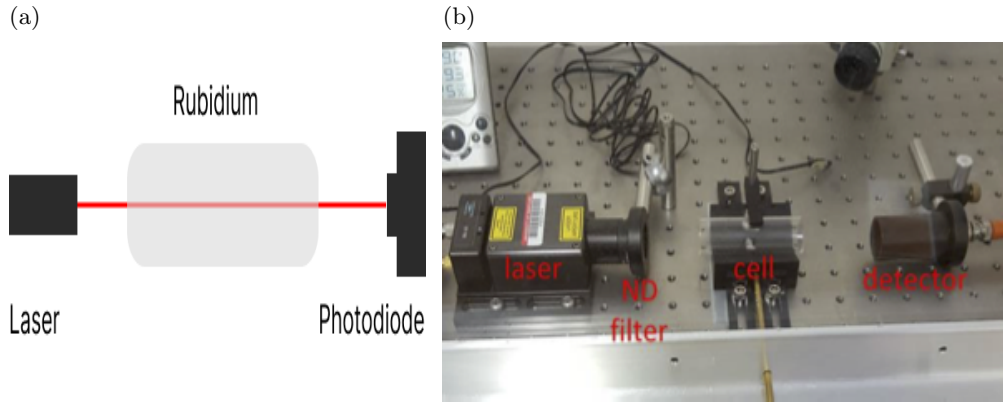


Figure 1: (a) Diagram of setup and (b) Photo of setup [6].

In this experiment, we are holding the temperature of the laser constant at a housing temperature of 25.5°C and operating temperature of 27.4°C [6]. Additional characteristics of the laser made to adjust the output to 780.24nm were performed by Vescent Photonics [6] and described in *Table 1*. The rubidium cell is constructed of a Pyrex tube which is evacuated. The laser traverses the cell

Table 1: Laser parameters [6]

<i>Type</i>	Distributed feedback (DBR)
<i>Wavelength</i>	780.24nm
<i>Light</i>	Infrared
<i>Len(s)</i>	Aspheric + 0.55 NA lenses
<i>Optical isolator</i>	35 dB
<i>Output power (initial)</i>	40 mW
<i>Output power (filtered)</i>	$\ll 1\text{ mW}$
<i>Neutral density filter</i>	ND=3.0
<i>Temperature (housing)</i>	25.5°C
<i>Temperature (operating)</i>	27.4°C

before reaching the photodiode. The signal from the photodiode is then amplified with a gain of $10^4 V/A$ before being sent to an oscilloscope where it is recorded.

This experiment is conducted at room temperature and therefore the atoms in the cell will be in some thermal motion [6]. The Maxwell-Boltzmann Distribution, equation (3), describes the probability that any given gas molecule in an ideal gas will be moving at a specific velocity [5].

$$P(v)dv = \left(\frac{M}{2\pi k_B T}\right)^{1/2} \exp\left(-\frac{Mv^2}{2k_B T}\right)dv \quad (3)$$

The velocity of this thermal motion, v , can be taken to be much less than the speed of light, c . Considering only the components of velocity which move along the axis of the beam, v_z , the effects of Special Relativity will give rise to a Doppler shift in the observed resonance frequencies from the reference frame of the laser [6]. This results in a distribution of resonance frequencies observed from the frame of the laser. Atoms moving towards the beam will have resonance frequencies above the values predicted by theory, while atoms moving away from the beam will have resonance frequencies lower than theory [6]. Equation (4) describes the correction to the resonance frequencies, f_L , from the laser reference frame.

$$f_L = f_0\left(1 + \frac{v_z}{c}\right) \quad (4)$$

By solving for v_z and substituting the result into equation (3), we obtain a relationship for the distribution of resonance frequencies.

$$P(f_L)df_L = \frac{2}{\delta\sqrt{\pi}} \exp\left(-4\frac{(f_L - f_0)^2}{\delta^2}\right)df_L \quad (5)$$

Where $\delta = 2\frac{f_0}{c}\sqrt{\frac{2k_B T}{M}}$. By relating δ to the FWHM of the resonance frequency distributions we observe, we can obtain a relationship to measure temperature.

$$T = \left(\frac{\delta c}{2f_0}\right)^2 \frac{M}{2k_B} = \left(\frac{\sigma c}{f_0}\right)^2 \frac{M}{k_B} \quad (6)$$

The frequency, f_0 , in this relation is different for each isotope and energy transition. *Table 2* shows the respective frequencies.

Table 2: Resonance frequencies (GHz/s) [7, 8]

^{85}Rb F2	384.231264888
^{85}Rb F3	384.228229157
^{87}Rb F1	384.232563005
^{87}Rb F2	384.225728324

It is worth noting the importance of the reference frame in this experiment. Considerations of Special Relativity require selection of a reference frame to carry out calculations. From the reference frame of the atom moving with a velocity to or from the laser beam, it will only absorb resonance frequencies precisely equivalent to the theoretical values predicted in equation (2). In the reference frame of the atom, everything else is moving with respect to it. Since we are collecting data directly from the laser, the reference frame of this experiment is that of the laser and therefore Doppler shift considerations must be made. From this point on, it may be assumed any and all calculations are made from the reference frame of the laser.

This experiment consists of two parts. The first part maps the current to the photodiode signal to identify the current levels where the atoms in the Rb cell experience resonance. The second part focuses on the identified resonance current levels and attaches a function generator to the laser to oscillate the current around the resonance frequencies. Measurements in the second part of the experiment are made with the rubidium cell and without the rubidium cell to allow background adjustments in the data analysis. After this adjustment, we can obtain a measurement for the average temperature of the atoms.

3 Measurement and Data Analysis

3.1 Map of Laser Output

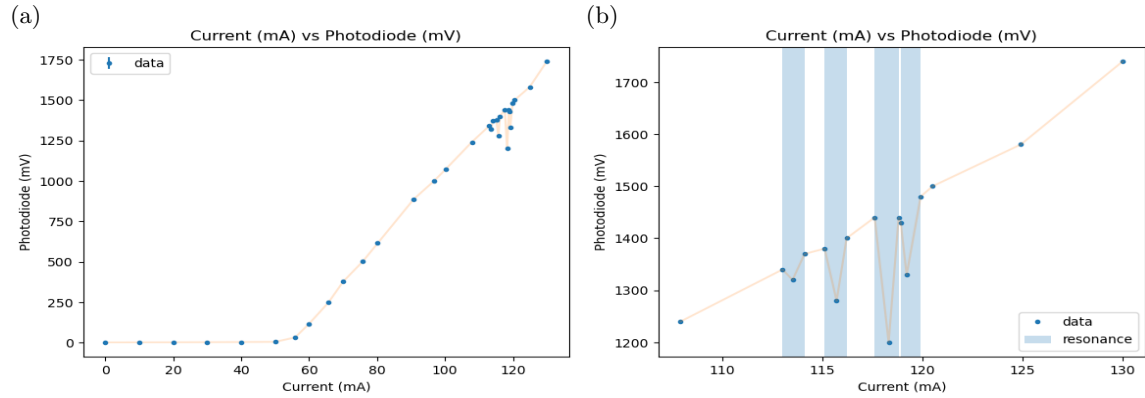


Figure 2: Results of Part One (a) Full map of photodiode and (b) Resonance map of photodiode

Measurements from the first part of the experiment were made by hand observing the voltage readings from the oscilloscope. Starting from a current of 0mA , voltage readings were made in increments of 10mA with extra measurements made at resonance levels. *Figure 2* shows the relationship between current and voltage to be linear, with drops in voltage when the isotopes experience resonance. It is interesting to note the threshold currency of the laser diode, the point at which the laser power begins to show this linear relation [3]. *Table 3* shows key values obtained from this part of the experiment.

Table 3: Intensity map of laser diode

Current (mA)	Voltage (mV)	Comments
55.9	32.1	Threshold currency
113.5	1320	Peak of $^{87}\text{RbF2}$ resonance
115.7	1280	Peak of $^{85}\text{RbF3}$ resonance
118.3	1200	Peak of $^{85}\text{RbF2}$ resonance
119.2	1330	Peak of $^{87}\text{RbF1}$ resonance

Results of this part of the experiment identified the current levels at which resonance occurred. A general distribution was observed at resonance current levels in accordance with theory and shown in *Figure 2b*.

Finally, uncertainty measurements were recorded in this part of the lab by observing the minimum and maximum mean values of the photodiode intensity on the oscilloscope. They are not reliable and were not used in any part of the following analysis.

3.2 Analysis of Absorption Signal

To analyze the absorption signal, the laser intensity was recorded after the laser traversed the *Rb* cell (the "signal" data). The *Rb* cell was then removed and the laser intensity was measured again (the "background" data). There were three trials recorded for signal data and two trials recorded for the background data. In the following analysis, *Trial 3* is used for the signal data and *Trial 2* is used for the background data. This selection was made based on the alignment of the time scale between the two measurements.

Due to Fresnel reflections on the glass surface of the *Rb* cell, the intensity of the laser will drop by a factor, X , before reaching the photodiode [6]. By comparing the linear components of the signal data with the background data, X can be calculated using equation (7).

$$m_{bg} = X m_{cell} \rightarrow X = \frac{m_{bg}}{m_{cell}} \quad (7)$$

The signal data can then be corrected by dividing the intensity of the background by X , and subtracting the adjusted background from the signal which removes the linear slope from the data. The signal data can then be inverted to reveal the plot in *Figure 3b*. The uncertainty in X is

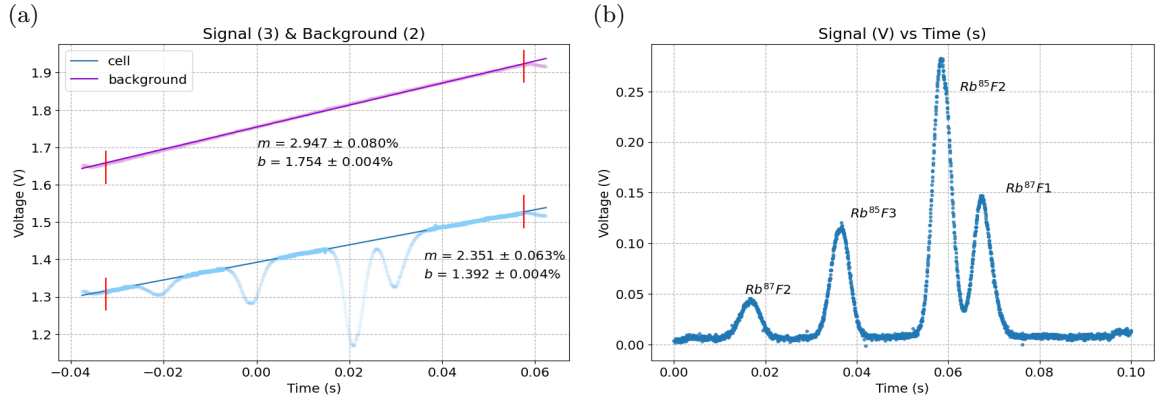


Figure 3: First part of signal analysis. **(a) Linear fit of background and signal data with uncertainties.** The red lines indicate where the data was cut to avoid complications in the linear fit. The final values for the slopes were $m_{bg} = 2.947 \pm 0.08\%$ and $m_{sig} = 2.351 \pm 0.06\%$. The uncertainties were derived from the *stderr* parameter returned from the linear regression fit performed in python. **(b) Final output after multiplying the signal data by X and subtracting the background.** The time axis is shifted right by 0.0376s to make the entire axis positive.

calculated using propagation of errors from the σ of m_{bg}, m_{sig} . A detailed derivation is provided in *Section 5.1.1*.

$$X = 1.25 \pm 0.1\%$$

The data shows approximately a 20% drop in the intensity of the photodiode signal as a result of Fresnel reflections. The labeling of the peaks was performed using intuition about the population of ^{87}Rb and ^{85}Rb , as well as the relative spacing between their respective peaks according to theory [6].

A comment on uncertainty up to this point in the analysis is worth mentioning. The uncertainty in the voltage readings can be taken to be 0.002mV , which was obtained from the linear fit performed in *Figure 3a*. This has little impact on the rest of the analysis as it is entirely focused on the horizontal axis and identifying a proper conversion from the axis in time (s) to frequency (Hz).

3.3 Conversion to frequency axis

The conversion to the frequency axis is where the largest source of uncertainty appears. There is a core assumption being made in the analysis which is not sure to be correct. First, I assume that the peaks in the graph correspond to the known resonance frequencies for the isotopes in the ground state, shown in *Table 2*.

This assumption is core to the model, as it assumes that there is no shift in the resonance frequencies for the energy transition levels for the largest majority of atoms. Fundamentally, I feel this assumption is wrong. However, we assume $v_c \ll c$ in equation (4), so we know the shift in frequency will be close to negligible.

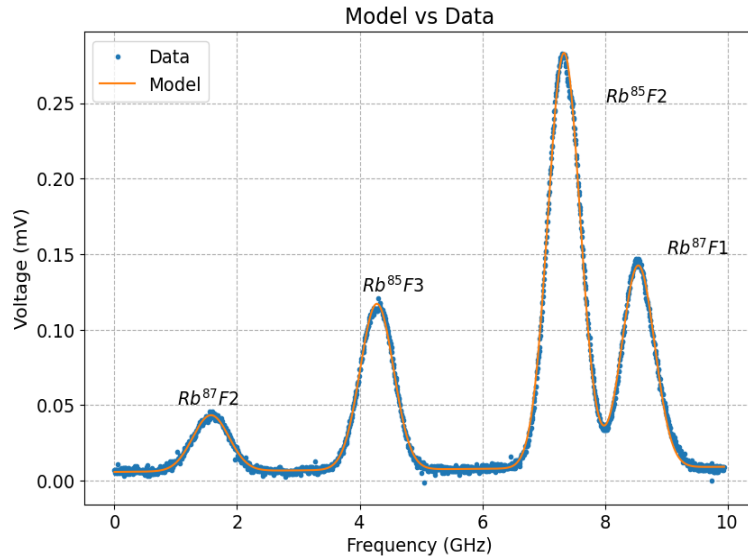


Figure 4: Model overlaying data. The fit $\chi^2_\nu = 1.14$ indicating a strong agreement with the data. The model was calculated with four Gaussian curves and a linear background noise which accounted for the points in between the Gaussian's.

This model enabled calculation of the FWHM of each Gaussian peak and therefore a temperature reading for each isotope according to equation (6). Once a temperature for each isotope was obtained, a weighted average was applied to calculate a final mean temperature for the *Rb* vapor. *Section 5.1.3* shows the equation used to calculate the weighted average and the uncertainty in the weighted

average. Justification of using a weighted average in this case as opposed to a unweighted average follows from the logic that there is no reason to assume the isotopes would have any difference in temperature beyond some very small fluctuations. Any discrepancy between the temperature values is then due to some uncertainty, which justifies the use of the weighted average. The source of uncertainty which causes a discrepancy between the temperature values for each isotope is not clear.

The final temperature readings for the two methods of calculating the time to frequency conversion are listed below in *Table 4*. A brief explanation of the methodologies is additionally in *Section 3.3.1* and *Section 3.3.2*. The values are much higher than expected, which I attribute to a systematic error in the time to frequency conversion factor. I was not able to calculate a value for this error. Additional sources of error include the spectral width of the laser beam, background noise from the environment effecting the photodiode measurements at low voltages and equipment degradation. The temperature in the lab during the day of measurement was $23.9^{\circ}C = 297.05K$. This large difference between the temperature of the environment and the obtained values in *Table 4* caused me great trouble, and I failed in determining the source of such error.

Table 4: Final Temperature Calculations

Method	Temperature (K)	$t(s) \rightarrow f(Hz)$ Factor
1	$439 \pm 42 (K)$	$137.21 (GHz/s)$
2	$439 \pm 42 (K)$	$132.39 (GHz/s)$

3.3.1 Method 1

Assumption of peaks corresponding to the values in *Table 2*. For each peak, take the difference in known frequency between the peaks and divide it by the difference in seconds between the two peaks as shown in equation (8). The final calculation is an average over the three values obtained.

$$t \rightarrow f = \frac{1}{3} \sum \frac{\Delta f}{\Delta t} \quad (8)$$

3.3.2 Method 2

Assumption of peaks corresponding to the values in *Table 2*. Take the difference between the two peaks of the same isotope (difference between peak of ^{87}Rb and ^{85}Rb) and divide it by the difference in seconds between the two peaks as shown in equation, similar to equation (8) but with a factor of $\frac{1}{2}$ out front as opposed to $\frac{1}{3}$.

4 Conclusion

In conclusion, the final temperature reading of $439 \pm 42 (K)$ was in strong disagreement with expectations. Though I would not expect the temperature in the cell to be exactly room temperature ($297.05K$), I certainly would expect it to be within a margin of $\pm 25\%$. The difference between the values is $25\% - 38\%$ using the extreme values of the temperature reading. This great discrepancy has led me to conclude that there is a large source of systematic error which I could not account for. I hope to discover this error in my future work surrounding this experiment and hope to obtain a more reasonable value for temperature. The sections below outline the unsuccessful methodologies I used in my efforts to obtain a lower temperature for future reference to scientists who explore this experiment.

4.1 What did not work

While conducting analysis it quickly became clear that high temperature readings were a result of the σ from the Gaussian fits and the position of f_0 , or time to frequency conversion factor. In order to determine what reasonable values would look like for each variable, I ran several mock trials and measured the output temperature readings. I determined a reasonable $\sigma \approx 0.25GHz$ and a reasonable time to frequency factor $\approx 110GHz/s$. Each of the following methods were unsuccessful at achieving lower values.

4.1.1 Not adjusting for background

The first idea was to not subtract the intensity factor, as done in *Figure 3a*, and fit the data as is. This was attempted by inverting the signal data and performing a model fit with four Gaussian curves and a linear background. This method did result in different values than obtained from the model fit used in *Section 3.2*, however the values were high and the $\chi^2_\nu \gg 1$, indicating disagreement the model disagreed with the data.

4.1.2 Voltage to Frequency Relationship

After fitting the Gaussian's and obtaining the model in *Section 3.2*, it was not possible to obtain lower values for σ for each isotope. It was then concluded the frequency to time conversion factor would need to be reduced. The first idea was to avoid using the signal data entirely to calculate this factor and rely solely on the linear fit of the background data. Since the voltage of the background data was increasing linearly, the goal was to convert the voltage readings to values of energy, and then to frequency. From this, I would be able to derive the total range of frequency traversed in the experiment from total range of voltage. The problem that could not be overcome with this method is the conversion of voltage to energy. Voltage has units of (E/C), the charge of which was unknown. Being unable to convert the charge into any known variable, this method had to be abandoned. Additionally, the signal amplifier of 10^4 would need to be accounted for in order to get a correct value for frequency. A short calculation was made to see what current level would yield a reasonable value for frequency, and it was extremely low. Ultimately, the unknown current is a property of the photodiode, which was not recorded.

4.1.3 Utilizing a minimize function to optimize the conversion factor at the best possible value

The final idea was to use a minimize function (such as in the scipy python library) to find an optimal factor for the time to frequency conversion. Equation (9) explains this idea mathematically.

$$\alpha \left| \frac{\Delta t_{Rb87}}{\Delta f_{0_{Rb87}}} - \frac{\Delta t_{Rb85}}{\Delta f_{0_{Rb85}}} \right| = 0 \quad (9)$$

This method does not work since the equation above is linear so technically you could choose α to be whatever you wanted to be most optimal. I hoped to find some reasonable way around this limitation and use a minimize function to optimize to some value, but since there was not a listed value for theory, this was not possible. In the end I had to scratch this method as well.

Question 1

When the laser was tuned to a *Rb* resonance, the photodiode signal dropped significantly in power. This occurs as a result of atomic absorption of the *Rb* atom when the beam carries a frequency

equal to the energy difference between the ground state and excited state of the atom. When the atom absorbs a photon from the beam, it instantaneously decays back to the ground state and emits another photon of the same frequency which it absorbed [1]. However, the photon emission occurs in a random direction and therefore will not contribute to the signal of the original laser beam. For this reason, the photodiode signal drops when the frequency of the beam is at a resonance frequency of the atoms.

Question 2

I expect the peaks to be Gaussian because of the Doppler broadening effect. The Doppler broadening effect is a result of the distribution in velocities of the *Rb* atoms at room temperature. The velocity distribution follows a Maxwellian distribution, described in equation (3), which takes a Gaussian form. As such, I expect the frequency at which the *Rb* atoms experience resonance to be resemble a distribution around a frequency as opposed to a single peak. Additionally, while I mapped the photodiode in the initial measurements of the experiment, I recorded the start, stop and peak current levels at which the resonance occurred. Plotting these resemble a Gaussian distribution as seen in *Figure 2b*.

Question 3

The temperature I read off from the thermometer was (297.05K). As mentioned in the conclusion, there is a huge discrepancy between my calculated values and the room temperature. The best idea I have as to why this may be the case is perhaps heat from the resonance frequency radiation has heated the cell over time. I took several measurements and the laser had oscillated around resonance many times by the time I took *Trial 3*. I have no idea how that would contribute a 100K+ discrepancy, and all other sources of uncertainty seem to be way too small to contribute meaningfully to that value as well. I battled this question for well over a week and I still have no idea why the values disagree so much.

Question 4

Doppler broadening occurs as a result of thermal motion in atoms at room temperature. When we conduct experiments in spectroscopy and probe atoms with lasers, this thermal motion broadens the resolution of our results as atoms will be moving in various directions in relation to the laser and therefore experience energy transitions at a distribution of frequencies as opposed to a single frequency. "Doppler-free" absorption spectroscopy is a technique which improves the resolution of spectral measurements by several orders of magnitude. The technique uses two laser beams, a pump and a probe beam, tuned to the same frequency and traveling in opposite directions. Since the pump and probe beam are traveling in opposite directions, they will excite different atoms as a result of the doppler shift. When the lasers are tuned to the resonance frequency of atoms with no thermal motion (theoretically), they will interact with the same atoms as there will be no Doppler shift in this case. The pump beam, operating at a significantly higher intensity than the probe beam, will "depopulate" this group of atoms by exciting the majority them. By measuring the absorption signal of the probe beam, we will see a sharp and significant drop at this frequency due to the depopulation by the pump. This dip is referred to as the Lamb Dip and the width of the Lamb dip can be described as the natural width of the transition state[4]. By relating this width to the lifetime of the state, we can get a measurement for the frequency of the absorption for the sample

by equation (10) where ν is the frequency and Γ is the lifetime of the excited state.

$$\delta\nu = \frac{\Gamma}{2\pi} \quad (10)$$

This, in summary, is the basis of the Doppler-Free absorption spectroscopy as the width of the Lamb dip is significantly more narrow than that achieved in normal absorption spectroscopy measurements.

4.2 Future Improvements

Besides performing Doppler-Free spectroscopy to improve this experiment, which I am not sure would result in better values for the temperature reading, I think the largest improvement in my understanding would have been to conduct the experiment with multiple temperatures for the cell. A thought model I experimented with was to consider how the Gaussian distributions would change as I raised and lowered the temperature in the cell, and how that would change f_0 for each of the peaks. I had a visual understanding, however I never really came to understand how f_0 would be shifted from the values predicted by theory, meaning where the peak of the Gaussian would be on the frequency axis. Knowing this would have made all the difference in my measurements.

5 Appendix

5.1 Derivations

5.1.1 Slope factor

Uncertainty

$$\begin{aligned} \sigma_X &= \sqrt{\left(\frac{\partial}{\partial m_{bg}} \sigma_{m_{bg}}\right)^2 + \left(\frac{\partial}{\partial m_{cell}} \sigma_{m_{cell}}\right)^2} \\ &= \sqrt{\left(\frac{1}{m_{cell}} \sigma_{m_{bg}}\right)^2 + \left(\frac{-m_{bg}}{m_{slope}^2} \sigma_{m_{cell}}\right)^2} \end{aligned} \quad (11)$$

5.1.2 Temperature

Uncertainty

$$\begin{aligned} \sigma_T &= \sqrt{\left(\frac{\partial}{\partial f_0} \sigma_{f_0}\right)^2 + \left(\frac{\partial}{\partial \sigma} \sigma_{\sigma}\right)^2} \\ &= \sqrt{\left(\frac{2c^2 \sigma^2 M}{k_B f_0^3} \sigma_{f_0}\right)^2 + \left(\frac{2\sigma c^2 M}{k_B f_0^2} \sigma_{\sigma}\right)^2} \end{aligned} \quad (12)$$

5.1.3 Weighted Average [9]

Weight

$$w_i = \frac{1}{\sigma_i^2} \quad (13)$$

Normalize weights

$$w'_i = \frac{w_i}{\sum_{j=1}^n w_j} \quad (14)$$

Weighted average

$$\bar{x} = \sum_{i=1}^n w'_i x_i \quad (15)$$

Uncertainty in weighted average

$$\sigma_{\bar{x}} = \sigma \sqrt{\sum_{i=1}^n (w'_i)^2} \quad (16)$$

where σ is the standard deviation of the temperature values.

References

- [1] Doppler free saturated absorption spectroscopy. http://instructor.physics.lsa.umich.edu/adv-labs/Doppler_Free_Spectroscopy/DopplerFree.pdf.
- [2] Rubidium - element information, properties and uses: Periodic table. <https://www.rsc.org/periodic-table/element/37/rubidium>.
- [3] Fosco Connect. Laser diode characteristics. <https://www.fiberoptics4sale.com/blogs/archive-posts/95047046-laser-diode-characteristics>.
- [4] John Brandenberger. Doppler-free spectroscopy. <http://web.mit.edu/8.13/www/JLExperiments/JLExp48.pdf>, 2012.
- [5] Northwestern. The maxwell-boltzmann distribution. <https://faculty.wcas.northwestern.edu/infocom/Ideas/mbdist.html>.
- [6] University of Maryland. Hyperfine structure of rubidium. <http://www2.physics.umd.edu/~beise/public/classes/p405/manual/Spring2009/Phys405-Chapter5.pdf>.
- [7] Daniel Adam Steck. Rubidium 85 d line data. <https://steck.us/alkalidata/rubidium85numbers.pdf>, 2001.
- [8] Daniel Adam Steck. Rubidium 87 d line data. <https://steck.us/alkalidata/rubidium87numbers.pdf>, 2001.
- [9] Wikipedia contributors. Weighted arithmetic mean. https://en.wikipedia.org/w/index.php?title=Weighted_arithmetic_mean&oldid=1146068450, 2023. [Online; accessed 29-March-2023].